CONCEPT OF SPECTRUM-SIGNAL TRANSFORMATION

Aleksandar Tasic and Wouter A. Serdijn

Delft University of Technology, Department of ITS
Electronics Research Laboratory, UbiCom Research Program
Mekelweg 4, 2628 CD Delft, The Netherlands
Phone: +31 (0)15 278 9423 Fax: +31 (0)15 278 5922
E-mail: a.tasic|w.a.serdijn@its.tudelft.nl

ABSTRACT

So far, there have been introduced many front-end studies, but most of them fail to present, in a consistent way, how the signals are transformed throughout the front-end itself. In this paper, it is intended to introduce a unique presentation of spectrum and signal transformation within RF front-ends. This approach should help researches to have better insight into the high-level modeling and characterization of RF front-ends and accordingly lead to new design strategies.

1. INTRODUCTION

For the last few decades, if it is about proposing new architectures, there haven't been many significant breakthroughs in the field of the radio frequency front-end design, as almost all the time two basic structures – high and zero IF – and some slight variations of theirs have been exploited. Even though the number of different topologies is very small, the high-level front-end characterization lacks an unique presentation, which in turn prevents researchers from even dare thinking of new strategies and approaches in the area of analog radio frequency front-end design.

In most papers dealing with any aspect of RF front-ends, the high-level description in the form of signal and spectrum presentation is either intentionally or accidentally skipped. In this paper, this issue will be deliberately addressed, as without a complete understanding of how the signals and their spectra are shaped throughout the front-end, it is not possible to grasp any other concept encountered in the jungle named RF front-end design.

This paper is divided in seven sections, each emphasizing one of the important aspects of the high-level characterization of the front-end architectures, for the sake of brevity simplified to the level of mixer-oscillator structures. The following section deals with signal transformation, while in Section 3 the spectrum transformation as applied to the front-end is analyzed. Section 4 introduces the concept of different mixer-local oscillator models and subsequently, using their specific properties, it provides a guidance for an all-encompassing analysis of signal and spectrum transformations. In Section 5, the resulting model is extended to be used for the image-rejection ratio calculations, which can straightforwardly be used for characterizing models of any complexity. In Section 6, the proposed model is applied to the example of image rejection mixer architecture.

2. SIGNAL TRANSFORMATION

Let us consider a simple quadrature downconversion structure as depicted in Fig. 1a.

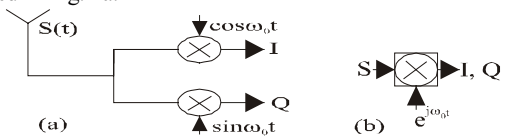

Fig. 1 (a) Quadrature downconverter. (b) Symbol.

The input signal denoted as *S(t)* is defined in Eq. (1), where *A* and *B* are quadrature components of the desired signal at ω_{RF}, and *C* and *D* quadrature components of the image signal at ω_{IM}. Its spectrum is shown in Fig. 2, where ω_{IF} is the intermediate frequency and ω_0 the LO frequency.

$$S(t) = A\cos\omega_{RF}t - B\sin\omega_{RF}t + C\cos\omega_{IM}t - D\sin\omega_{IM}t \qquad (1)$$

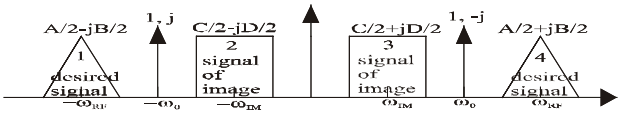

Fig. 2 Spectra of the desired, the mirror and the LO signal.

Mathematical representation of the signal transformation is obtained as follows:

$$\omega_{IF} = \omega_{RF} - \omega_0$$

$$2\cos\omega_0 t = e^{j\omega_0 t} + e^{-j\omega_0 t}\ ,\ \ j2\sin\omega_0 t = e^{j\omega_0 t} - e^{-j\omega_0 t}$$

$$R = \sqrt{A^2 + B^2}\ ,\theta = \text{a tan}\frac{B}{A},\ \text{M} = \sqrt{C^2 + D^2}\ ,\ \psi = \text{a tan}\frac{D}{C}$$

As the complex presentation of the input signal *S(t)* is:

$$2S(t) = (A + jB)e^{j\omega_{RF}t} + (A - jB)e^{-j\omega_{RF}t} + (C + jD)e^{j\omega_{IM}t} + (C - jD)e^{-j\omega_{IM}t}$$

$$2S(t) = R\cdot e^{j(\omega_{RF}t+\theta)} + R\cdot e^{-j(\omega_{RF}t+\theta)} + M\cdot e^{j(\omega_{IM}t+\psi)} + M\cdot e^{-j(\omega_{IM}t+\psi)} \qquad (2)$$

the in-phase (I) and the quadrature-phase (Q) component equal:

$$2I = LowFiltered[S(t)(e^{j\omega_0 t} + e^{-j\omega_0 t})]$$
$$2I = R\cdot\cos(\omega_{IF}t + \theta) + M\cdot\cos(\omega_{IF} - \psi) \qquad (3)$$

$$2Q = LowFiltered[Sa(t)(e^{j\omega_0 t} - e^{-j\omega_0 t})]$$
$$2Q = -R\cdot\sin(\omega_{IF}t + \theta) + M\cdot\sin(\omega_{IF} - \psi) \qquad (4)$$

Now, we can consider the converted signal as a whole, consisting of I and Q components, in the form:

$$2(I + jQ) = (A - jB)e^{-j\omega_{IF}t} + (C\text{-}jD)e^{j\omega_{IF}t} \qquad (5)$$

This expression will be used as the base for the subsequent characterization of the front-end models. As all the signals are actually real, the real value of the signal equals:

$$2\,\mathrm{Re}\{I + jQ\} = A\cos\omega_{IF}t - B\sin\omega_{IF}t + C\cos\omega_{IF}t + D\sin\omega_{IF}t \quad (6)$$

The resulting spectra of the desired signal and image are at the negative and positive frequencies respectively – Fig. 3.

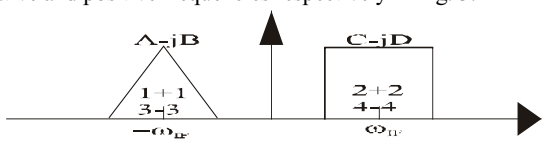

Fig. 3 Spectrum of the input signal after downconversion.

As seen from Fig. 3, the signal is characterized by both spectrum position and its exact content in the form of orthogonal components *A* and *B*. After downconversion, the signal is still detectable, consisting of corresponding I-phase and Q-phase components *A-jB*. Its real value is the same as that of the signal entering the receiver $A\cos\omega_{RF}t - B\sin\omega_{RF}t$.

3. SPECTRUM TRANSFORMATION

Let us now determine how the spectrum is transformed by the down-conversion process. For the sake of simplicity, filters are omitted in all down-converter models throughout this paper, but it is assumed that each portion of downconversion is followed by a portion of filtering (low pass or band-pass). This means that only down-converted parts of the spectrum are taken into account.

To have better understanding of the down-conversion process, we will independently investigate I and Q paths, i.e., downconversion with $\sin\omega_O t$ and $\cos\omega_O t$, respectively. The spectrum of the input signal together with the spectrum of the local oscillator (LO) signal are shown in Fig. 2.

As downconversion is equivalent to convolution of spectral representation of $\cos\omega_O t$ and $\sin\omega_O t$ with the spectrum of the input signal, the corresponding output spectrum for I and Q paths is as given in Fig. 4.

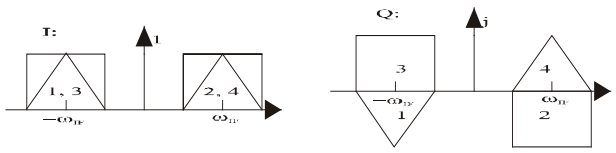

Fig. 4 Spectra of I and Q channels.

After the transformation of the Q-spectrum into the *jQ* one, as has been done with the mathematical representation of the signal so as to maintain the complex notation, when both I and Q spectra are "real", the resulting spectrum can be obtained after summation of the spectra of corresponding orthogonal components, *I+jQ* (see Fig. 3).

Thus, we have derived an explicit relation between the spectral and mathematical representation of the signal. To be even more specific, let us stress that after frequency conversion the desired signal is at frequency $-\omega_{IF}$ and presented in the form $(A\text{-}jB)e^{-j\omega IFt}$, where *A-jB* is just a mathematical interpretation of quadrature components of the signal, which is in fact "real" and of the same form as given by Eq. (6).

Not surprisingly, this form is the same as of the signal entering the system. Furthermore, by presenting signal in this way *(A-jB),* more useful information characterizing the signal is available. The components of the signal can still be distinguished between each other as signal orthogonality is preserved. To keep track of both spectrum and signal content, one might straightforwardly use the presentation shown in Fig. 3 - in this paper called *spectrum-signal presentation*.

4. MIXER-LOCAL OSCILLATOR MODELS

In order to bring more order and consistence in the modeling of the RF front-end architectures, the models of *real_mixer-LO*, *single_complex_mixer-LO* and *double_complex_mixer-LO* are introduced. These models are meant to simplify the corresponding mixer-local oscillator structures for the purpose of facilitating the spectral analysis of the RF front-ends. Subsequently, it is examined how the spectrum of the input signal is transformed in the real front-end architectures.

4.1 Real_mixer-LO

As in the case of the superheterodyne architectures, it is not possible to distinguish between the desired signal and image after first down-conversion without previous filtering (image-reject filters). This is shown in Figs. 2 and 4 (I path).

4.2 Single_complex_mixer-LO

In order to take the advantage of using single_complex_mixer-LO (symbol is given in Fig. 1b) for the purpose of easier graphical and mathematical presentation, it is necessary to first transform all the spectral components to either positive or negative frequencies. This is done because LO doesn't "see" the signal at both positive and negative frequencies. Illustration is given in Fig 5.

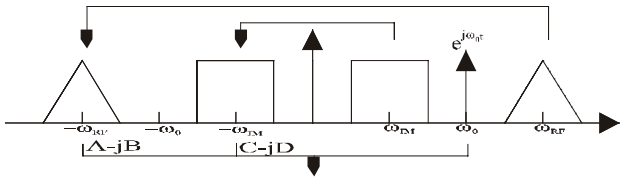

Fig. 5 Single_complex_mixer-LO (spectra).

The mathematical counterpart of this kind of presentation is explained as follows (for this purpose we are considering signal of the form (2) as the one entering the receiver).

Transformation of the components at the frequency ω_{RF} and ω_{IM} to $-\omega_{RF}$ and $-\omega_{IM}$ is, with respect to the signal content, equivalent to the summation of non-transformed and complement of the transformed parts. In this case it yields:

$$-\omega_{RF}: \ 1/2(A - jB) + 1/2\overline{(A + jB)} = A - jB$$
$$-\omega_{IM}: \ 1/2(C - jD) + 1/2\overline{(C + jD)} = C - jD$$

Knowing the signal content, we can play with the introduced single_complex_mixer-LO model (S_C_M-LO) and perform the transformation as shown in Fig. 5.

As explained in Section 2 (signal presentation) and Section 3 (spectral presentation), we can now easily follow how both the signal and its spectrum are being transformed.

4.3 Double_complex_mixer-LO

Let us now consider an even more complicated case in the form of the double quadrature downconverter, as shown in Figs. 6a and 6b.

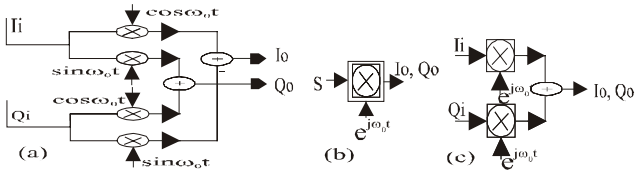

Fig. 6 Double_complex_mixer-LO (symbols).

Unlike S_C_M-LO, in a double_complex_mixer-LO model (D_C_M-LO), LO "sees" the signal at both positive and negative frequencies. In this case LO can be presented as $e^{j\omega t}$ [1] without any transformation of the spectrum. Fig. 7 shows the spectrum-signal form of downconversion from the intermediate frequency using the proposed D_C_M-LO model (first downconversion has already been done with simple quadrature downconverter).

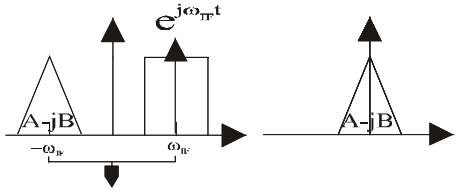

Fig. 7 Double_complex_mixer-LO (spectra).

This will be clarified through an all-encompassing spectral analysis of double quadrature downconverter model.

This structure can equivalently be represented using S_C_M-LO (Fig. 6c). Spectrum-signal form of the input signal is shown in Fig. 2, where the mathematical representation of the signal is allocated to each part of the spectrum according to the explanation from the previous sections (NB: in the context of transformation of the spectra, the term "signal" is actually referred to mathematical representation of the signal).

Before applying the analysis method introduced here, the signal is presented in such a way so that S_C_M-LO can straightforwardly be used.

$$(A-jB)e^{-j\omega_{IF}t} = \mathrm{Re}\{(A-jB)e^{-j\omega_{IF}t}\} - j\,\mathrm{Re}\{(B+jA)e^{-j\omega_{IF}t}\}$$
$$(C-jD)e^{j\omega_{IF}t} = \mathrm{Re}\{(C-jD)e^{j\omega_{IF}t}\} - j\,\mathrm{Re}\{(D+jC)e^{j\omega_{IF}t}\}$$

Without loss of generality, one might assume that first downconversion with S_C_M-LO has already been done and that spectrum-signal form at the intermediate frequency is as shown in Fig. 3.

Now, it is possible to transform the model of Fig. 3 into the one of Fig. 8, corresponding to the I and Q channels of the downconverted signal – Eq. (7).

$$\begin{aligned} I &= \mathrm{Re}\{(A-jB)e^{-j\omega_{IF}t}\} + \mathrm{Re}\{(C-jD)e^{j\omega_{IF}t}\} \\ Q &= \mathrm{Re}\{-(B+jA)e^{-j\omega_{IF}t}\} + \mathrm{Re}\{-(D+jC)e^{j\omega_{IF}t}\} \end{aligned} \quad (7)$$

As expected, the image is suppressed after the final downconversion. Also, as the resulting spectrum of Fig. 8 is the same as the resulting spectrum of Fig. 7, the validity of the proposed spectrum-signal form of D_C_M-LO model is proved.

Not intending to introduce additional confusion due to interchangeable use of signal presentation in real and complex form, here are some explanations with respect to this issue. All signals are real; complex notation is used only to keep track of orthogonal components of the signal. For example, $A+jB$ means

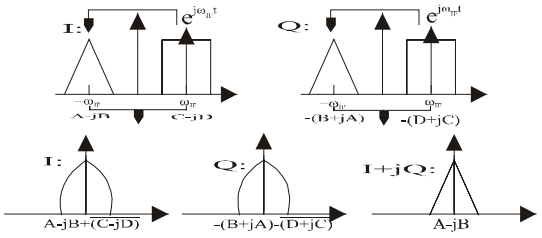

Fig. 8 D_C_M-LO using S_C_M-LO models (spectra).

that there is still information about signal A and signal B, while $A+B$ means that it is not possible to distinguish between them. To conclude this part, complex notation is used just as the abstraction of the signal in the RF front-ends.

With the advantage of double_complex_mixer-LO model we can manipulate using fairly simple forms of signals and spectra compared to spectrum-signal form of Fig. 8, or even more complicated analysis found in [2][3] and Figs. 2, 3, and 4 (what is more, in this case all the given transformations must be done twice, once for I and once for Q channel).

The simplicity of the spectrum-signal form of D_C_M-LO model is shown in Fig. 7.

Note that transformations of Fig. 5 are introduced so as to give more insight into the content of the signal, being together the desired and the mirror signal. If the same is applied to the spectrum-signal form of Fig. 3 the signal can be presented as

$$(A-jB)+\overline{(C-jD)} = A-jB+C+jD$$

This suggests that the phase sequences [4] of the desired signal and the signal of image are of different polarities. Owing to this property of the downconverted signals, the polyphase filters can distinguish between the positive and negative sequences, being the clockwise and counterclockwise phase order of the signals.

5. IRR MODEL

Straightforward use of the spectrum-signal transformation yields simple but accurate explanations of many phenomena related to the RF front-ends. As an example, we will evaluate the image-rejection-ratio IRR of a simple quadrature downconverter section.

First, let us denote ε and φ as amplitude and phase mismatch of the LO signal, as shown in Fig. 9.

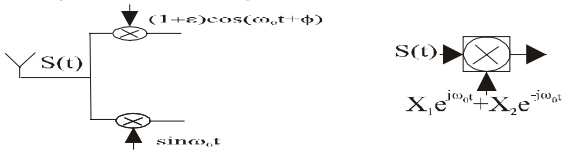

Fig. 9 IRR analysis model.

For LO signal it can be written:

$$(1+\varepsilon)\cos(\omega_0 t+\varphi) + j\sin\omega_0 t = [X_1(\varepsilon,\varphi)e^{j\omega_0 t} + X_2(\varepsilon,\varphi)e^{-j\omega_0 t}]$$
$$\begin{aligned} X_1(\varepsilon,\varphi) &= (1+\varepsilon)e^{j\varphi}+1 \\ X_2(\varepsilon,\varphi) &= (1+\varepsilon)e^{-j\varphi}-1 \end{aligned} \quad (8)$$

Without loss of generality, constants ½ and 2 that originate from the mixing with the LO signal can be left out, as we are only interested in the form of the signal, as well as the position of the spectrum, which are not affected using this simplification.

The IRR will first be found using strictly mathematical interpretation of the signals and subsequently it will be shown how

much simpler it is to come up with the same result using spectrum-signal notation.

In this particular case, S_C_M-LO is actually transformed into a kind of "distorted" real_mixer-LO, so that positive and negative frequency ranges are "seen" by the local oscillator (as, in fact, also occurs in Fig. 2).

If the low-filtered version of the output signal is:

$$OUT \propto RX_1(\varepsilon,\varphi)e^{-j(\omega_{IF}t+\theta)} + MX_2(\varepsilon,\varphi)e^{-j(\omega_{IF}t-\psi)} + RX_2(\varepsilon,\varphi)e^{j(\omega_{IF}t+\theta)} + MX_1(\varepsilon,\varphi)e^{j(\omega_{IF}t-\psi)} \quad (9)$$

then *IRR*, as the ratio of image and signal power at either positive or negative frequencies, can be calculated as:

$$IRR = \left|\frac{X_2(\varepsilon,\varphi)e^{-j(\omega_{IF}t-\psi)}}{X_1(\varepsilon,\varphi)e^{-j(\omega_{IF}t+\theta)}}\right|^2 = \left|\frac{-1+(1+\varepsilon)e^{-j\varphi}}{1+(1+\varepsilon)e^{j\varphi}}\right|^2$$
$$IRR = \frac{1-2(1+\varepsilon)\cos\varphi+(1+\varepsilon)^2}{1+2(1+\varepsilon)\cos\varphi+(1+\varepsilon)^2} \quad (10)$$

Not surprisingly, the well-known expression for the IRR [3] is obtained.

Let us now examine how powerful the all-encompassing spectrum-signal analysis method is when applied to the same downconverter architecture.

The complete story is given in Fig. 10, where the spectra of the desired signal, the image and LO are presented for the case before and after conversion.

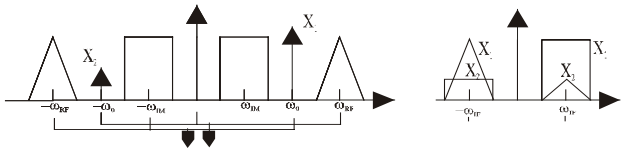

Fig. 10 Spectrum-signal transformation in case of mismatch.

From this figure, it is obvious to what extent the desired signal and the image are affected, so that *IRR* can therefore readily be calculated as in Eq. (10).

If one takes for example the case where ε_1 and φ_1 are amplitude and phase deviation of I-phase and ε_2 and φ_2 amplitude and phase deviation of Q-phase component of the LO signal, calculation of the IRR without the model proposed here will be very complicated. However, by means of the functions X_1 and X_2 of the form

$$X_1(\varepsilon_1,\varphi_1,\varepsilon_2,\varphi_2) = (1+\varepsilon_1)e^{j\varphi_1} + (1+\varepsilon_2)e^{j\varphi_2}$$
$$X_2(\varepsilon_1,\varphi_1,\varepsilon_2,\varphi_2) = (1+\varepsilon_1)e^{-j\varphi_1} - (1+\varepsilon_2)e^{-j\varphi_2} \quad (11)$$

as well as Eq. (10) and Fig. 10, *IRR* analysis appears to be much simpler.

6. AN ALL-ROUND EXAMPLE

To examine all the aspects of the proposed spectral analysis model – *spectrum-signal transformation,* we will use an all-round downconversion architecture being image-reject mixer architecture shown in Fig. 11a (standard form), and Fig. 11b (model as proposed here).

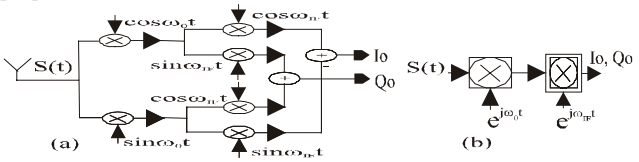

Fig. 11 Image-reject mixer architecture.

The spectrum-signal form is shown in Figs. 5 and 7.

For the purpose of IRR calculations, we are considering only part of the structure shown in Fig. 11 that is given in Fig. 12. Using the proposed method, a rather complex structure, especially for the calculation of *IRR* [4], boils down to an easy to understand and implement method, re-explained in Fig. 13, where the first downconversion is the same as in Fig. 10.

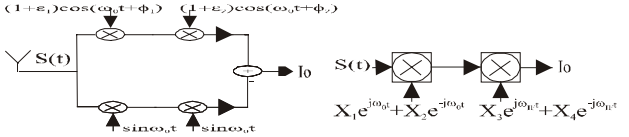

Fig. 12 IRR analysis model.

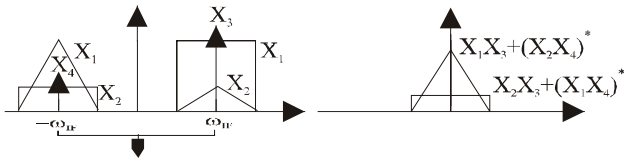

Fig. 13 Spectrum-signal transformation in case of mismatch.

As stated in Section 4, components that originate from different sides of the frequency axis are added in complement. The *IRR* is now calculated from Eq. (12) as [3]:

$$IRR = \left|\frac{X_2X_3 + \overline{X_1X_4}}{X_1X_3 + \overline{X_2X_4}}\right|^2$$
$$IRR = \frac{1-2(1+\varepsilon_1)(1+\varepsilon_2)\cos(\varphi_1-\varphi_2)+(1+\varepsilon_1)^2(1+\varepsilon_2)^2}{1+2(1+\varepsilon_1)(1+\varepsilon_2)\cos(\varphi_1+\varphi_2)+(1+\varepsilon_1)^2(1+\varepsilon_2)^2} \quad (12)$$

7. CONCLUSIONS

The complex signal technique combined together with the spectral presentation has proven to be a very powerful tool in both characterization and understanding the nature of RF front-ends, especially for researchers and designers entering the world of radio frequency microelectronics for the first time. Based on the existing models, an all-encompassing spectral analysis method is introduced in this paper, which addresses the issue of a consistent presentation of signal and its spectrum throughout the receive path of the RF front-ends. The proposed model relies on so-called spectrum-signal presentation offering a full interpretation of how both the signal and its spectrum are transformed when being downconverted from the high frequency range at the input up to the low frequency range at the output of the RF front-end.

8. REFERENCES

[1] J. Crols and M. Steyaert, *CMOS Wireless Transceiver Design.* Boston, Kluwer Academic Publishers, 1997.

[2] B. Razavi, *RF Microelectronics*, Upper Saddle River, NJ: Prentice Hall, 1998.

[3] J.C. Rudell *et al.*, "A 1.9-GHz Wide-Band IF Double Conversion CMOS Receiver for Cordless Telephone Applications*", IEEE Journal of Solid-State Circuits*, vol. 32, no. 12, pp. 2071-2088, December 1997.

[4] S. H. Galal, *et al.*, "RC Sequence Asymmetric Polyphase Networks for RF Integrated Transceivers", *IEEE Trans. CAS, Part II,* vol. 47, no. 1, pp. 18-27, January 2000.